Photoprocesses in AOT Reverse Micelles Containing Metalloporphyrins and Oligopeptides

M. Aoudia*,† and M. A. J. Rodgers‡

Department of Chemistry, College of Science, Sultan Qaboos University, P.O. Box 36, Al-Khod, Sultanate of Oman, and Center for Photochemical Science, Department of Chemistry, Bowling Green State University, Bowling Green, Ohio 43403

Received: September 30, 2002; In Final Form: April 7, 2003

Steady-state and time-resolved spectroscopy of two cationic metalloporphyrins—tetrakis(*N*-methyl-4-pyridyl)-porphyrin (Pd(II)TMPyP^{4+} and Zn(II)TMPy^{4+})—were studied in reverse micelles of AOT−heptane−H_2O in the absence, and presence, of oligopeptides containing tyrosine and tryptophan residues (K_2YL_2 and K_2WL_2). Ground-state absorption spectra for both porphyrins in reverse micelles at different water-to-surfactant molar ratio (w_0) values revealed a critical micellar water composition of $w_0 \approx 10$. Above this critical value, a w_0-independent red shift ($\Delta\lambda = 3.1$ nm) was observed, suggesting a similar aqueous porphyrin environment. Below $w_0 \approx 10$, a w_0-dependent blue shift was observed, indicating a porphyrin aqueous environment that is strongly related to the micellar size. At high micelle-water composition, the ground-state spectra never approached those observed in aqueous solution, strongly indicating that the porphyrin is preferentially solubilized in close vicinity of the H_2O−AOT molecular interface. Fluorescence emission from ZnTMPyP^{4+} in reverse micelles showed characteristics that were similar to those observed from ground-state absorption. Fluorescence emission from the single tryptophan residues of K_2WL_2 in aqueous solution and in reverse micelles suggested a solubilization site of the peptide near the micellar oil−water interface. This solubilization site was found to be dependent on w_0 below w_0 values of ∼10 (reflecting a different peptide microenvironment) and independent of w_0 above ∼10 (reflecting a similar peptide microenvironment). Flash photolysis experiments showed that, in the presence of a peptide in reverse micelles, Pd(II)TMPy^{4+} triplet decay was described by the sum of two exponential terms. The fast decay component for both oligopeptides was found to be independent of the peptide concentration and dependent on w_0. The slow decay component showed a linearly dependent increase in value, relative to increases in the peptide concentration. The fast contribution to the porphyrin triplet state T_1 decay was associated with electron transfer in a discrete micelle between the target moiety (tyrosine or tryptophan) and the photoexcited porphyrin molecule. The slow contribution of the decay was associated to molecular quenching during the micellar exchange process. The fast decay component was found to be independent of pH, suggesting a solubilization of the peptide molecule in a pH-independent environment near the oil−AOT molecular interface, where a portion of the heptane chain may extend into the water phase.

Introduction

Electron transfer within a protein matrix is critical to the function of a wide range of biological processes. Understanding the details of such reaction has generated considerable experimental[1−5] and theoretical[6−8] work. Recent investigations from this laboratory[9,10] reported on the photophysical processes in self-assembled ion-pair complexes between cationic metalloporphyrins, tetrakis(*N*-methyl-4-pyridyl)porphyrin (Pd(II)-TMPy^{4+} and Zn(II)TMPy^{4+}), and anionic pentapeptides consisting of a string of four glutamic acid residues terminated either by tyrosine (E_4Y) or tryptophan moieties (E_4W). These investigations provided evidence for photoinduced electron transfer from the ground state of the target aromatic amino acid (Y or W) to the metalloporphyrin triplet state and for the role played by the thermodynamic driving force ($\Delta G°$), the electronic coupling between the donor and acceptor (H_{AD}), the solvent reorganization energy (λ), and the local dynamics in the metalloporphyrin−peptide complex. This work was conducted in a buffered homogeneous aqueous system and, therefore, was far from being a realistic representation of the complexity of the heterogeneous nature inherent to biological membranes. In addition, it is well-known that the biological function of peptides is dependent on the structures they adopt on binding to cell surface receptors. In aqueous solution, they adopt multiple, rapidly interchanging conformational states and cannot generally be studied in their functional environment.[11] Thus, interest has shifted to the study of peptide conformations in association with model interfaces, such as lipid vesicles, surfactant micelles, and reverse micelles.[12−15] In this study, our aim is then to extend our earlier work[9] on photoinduced electron transfer in self-assembled oligopeptide−metalloporphyrin complexes in aqueous solution, to reverse micelles, which represent a useful alternative microheterogeneous medium to a standard homogeneous chemical system.

Reverse micelles, which are stable dispersions of water in nonpolar solvents, have been used extensively as biological membrane models to aid in the understanding of membrane chemistry.[16] By far, the most common system used in reverse micelle studies is the ternary mixture AOT−nonpolar−H_2O−

* Author to whom correspondence should be addressed. E-mail: aoudia@squ.edu.om.
† Sultan Qaboos University.
‡ Bowling Green State University.

10.1021/jp027106w CCC: $25.00
Published on Web 06/04/2003

solvent. AOT reverse micelles have been well characterized spectroscopically and thermodynamically. Techniques that have been used to probe these systems include, among others, light scattering, neutron scattering, and IR and NMR spectroscopy.[17−21] AOT micelles have the ability to solubilize large amounts of water and form highly spherical monodisperse droplets. The size of the micelles in a suspension are characterized by the water-to-surfactant molar ratio, w_0:

$$w_0 = \frac{[H_2O]}{[AOT]} \quad (1)$$

which has been shown to be directly proportional to the micellar radius.[22−24] "Dry" micelles ($w_0 = 0$) are slightly nonspherical; however, the micelles rapidly convert to a spherical shape upon the addition of small amounts of water. The smallest micelles possess a hydrodynamic radius of ~1.5 nm.[22] The aggregation number for the small micelles ($w_0 \leq 2$) is ~20 AOT molecules per micelle.[25] As more water is solubilized, the reverse micelles swell, incorporating large amounts of water ($w_0 \approx 50-70$) in discrete droplets.

The water pools inside the AOT reverse micelles possess some interesting properties. IR absorption spectroscopy showed that water molecules solubilized inside small micelles are in contact with and bound to the polar headgroups of the AOT molecules.[17−20] This inhibits their ability to form hydrogen bonds found in bulk water. As w_0 increases, the IR spectrum shifts toward that of bulk water, indicating that water molecules in the inner pool do form bulklike hydrogen bonds. Similar results have been observed using NMR spectroscopy.[21] In addition to these structural differences, experiments have revealed that the motion of water inside the micelles differ from that of bulk water.[26−29] Solvation dynamics was used to investigate the water motion via ultrafast time-resolved spectroscopy.[18−20,30−32] These experiments showed that the water inside the smallest micelles is completely immobilized, but a bulklike component appears as water is added and a water core forms. Furthermore, these investigations showed that the water dynamics in the smallest micelles (w_0 values up to 7) differs significantly from that of bulk water. However, the source of the mobility of water molecules is not fully understood. Hasegawa et al. used molecular probes to measure the microviscosity inside reverse micelles of varying sizes.[33] Their results indicated that the viscosity of water inside small micelles is greater than that in bulk water. The viscosity decreases dramatically up to $w_0 \approx 10$ and then decreases gradually as the micellar size increases.

Numerous kinetic studies have shown that the reaction rate constants are considerably altered in reverse micelles, compared to those in homogeneous solvents, and are dependent on the amount of solubilized water (w_0). Such an effect has been explained qualitatively, in terms of the state of the solubilized water in a reverse micellar core[32] and the change of the microviscosity[33] or polarity.[34] Localization and orientation of the reacting species were invoked, as well as their dilution, which induces an increase of the mean distance between them.[35] The effect of the sign of the interfacial charges was also reported.[36]

In the present study, our main objective was to use the oil−water reverse micelle interface as a model unit to mimic a biological membrane. Our primary hypothesis was that, in reverse micelles, tetracationic porphyrins such as those employed in our previous work[9] would be essentially solubilized within the water micellar pool. A suitable choice for peptides having an appropriate hydrophilic−lipophilic balance (HLB) and containing tyrosine (Y) or tryptophan (W) moieties within their molecular backbone was expected to ensure peptide localization at the micelle interface. Such a model would then place the oxidizable portion of the target residues (Y and W) near the porphyrin triplet state T_1. This would facilitate an eventual intramicellar electron transfer that is similar to that observed for self-assembled oligopeptide−metalloporphyrin complexes in aqueous solution.[9] Clearly, the coulombic interaction between the tetracationic porphyrin and the negatively charged AOT polar headgroups will certainly play a dominant role in setting up the possibility for an intramicellar electron-transfer event after photoexcitation of the porphyrin into its triplet state (T_1).

To materialize such a model, two pentapeptides—K_2YL_2 and K_2WL_2, where the tyrosine (Y) and tryptophan (W) residues are positioned between two lysines (L) and two leucines (K)—were synthesized using solid-phase peptide synthesis.[9] The criterion upon which leucine and lysine were selected as components of the peptide backbone was based on the significant difference between their HLB character. On the hydrophobicity scale of amino acids,[37] leucine is cited as the most hydrophobic (oil-soluble) amino acid, whereas lysine is mentioned as being the most hydrophilic. Therefore, in reverse micelles, one may anticipate that both peptides E_2YL_2 and E_2KL_2 will act as "cosurfactants" and tend to localize at the oil−water interface with leucine moieties projected toward the external oil phase and lysine moieties projected toward the interior phase (water phase). Furthermore, the presence of tyrosine and tryptophan in the peptide backbone may also play a key role in driving the peptide to localize at the micelle interface. It has been reported that, in integral membrane proteins, the aromatic acid residues W and Y tend to localize at the membrane−solution interface.[38−42] Other studies[43−46] showed that, in membrane proteins, tryptophan and tyrosine tend to cluster near the membrane−solution interface within the transmembrane region. A final beneficial feature relevant to this study is that porphyrins and oligopeptides can be used as their own probes to monitor the effect of the water-to-surfactant molar ratio (w_0) in solubilization sites.

Experimental Section

High-purity AOT (sodium bis(2-ethylhexyl) sulfosuccinate, 99%) was purchased from Fluka. Heptane (99%) was purchased from Aldrich. The two peptides (K_2YL_2) and (K_2WL_2) were synthesized via standard solid-phase synthesis, and the purification and characterization were performed using the procedure that has been fully described elsewhere.[9] Stock aqueous solutions of peptide and porphyrin were prepared in distilled water, and the pH was adjusted to 7.0 using HCl. Reverse micelles were prepared by mixing the requisite volume (a few microliters) of stock (peptide and porphyrin) solutions with a given amount of distilled water and 2.5 mL of AOT (6%) in heptane. The final volume was adjusted to 5 mL to yield a final concentration of AOT surfactant at 3% (w/v) in heptane. In some experiments, the pH of the injected water was varied by adding NaOH or HCl. The pH was measured with a calibrated Corning ion analyzer (model 250). Absorption spectra were recorded on a GBC model 918 UV−vis rapid scan spectrophotometer. Fluorescence spectra were measured with a Perkin−Elmer model LS-5B luminescence spectrometer.

Flash photolysis experiments were performed with the second harmonic (532 nm) of a Continuum Surelite I Q-switched Nd:YAG laser that provided 6-ns pulses. Transient absorbance was monitored at right angles to the laser excitation beam, using a

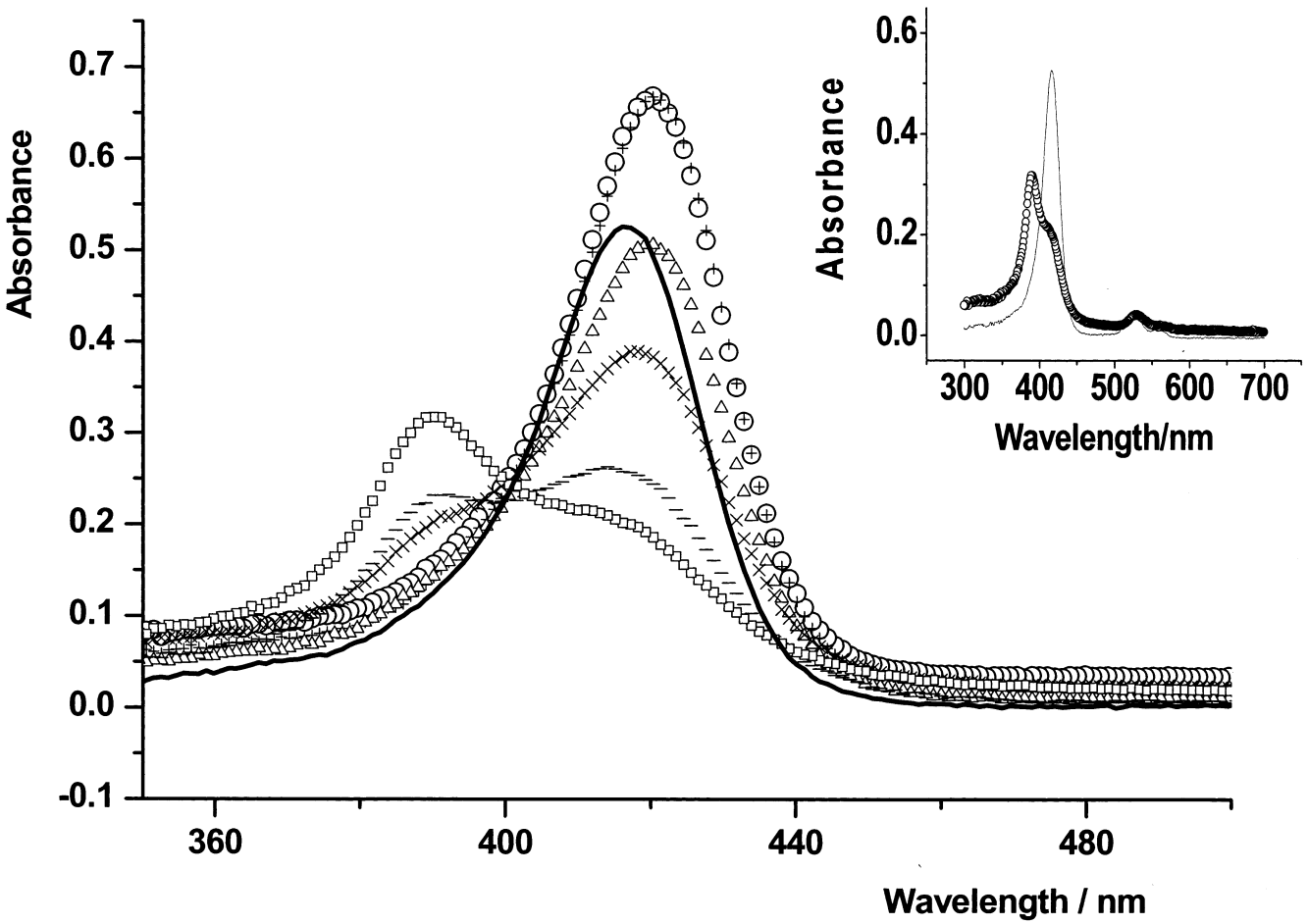

Figure 1. Ground-state absorption spectra of Pd(II)TMPy^{4+} (3.3 μM) in aqueous (pH = 7.0) solution (solid line) and in 3% AOT−heptane−H_2O reverse micelles at the following water-to-surfactant molar ratios, w_0: (○) 49.39, (+) 10.29, (△) 7.90, (×) 6.09, (−) 3.70, and (□) 1.64. Inset is the absorption spectra of Pd(II)TMPy^{4+} (3 μM) in aqueous (pH = 7.0) solution (solid line) and in 3% AOT−heptane−H_2O (dotted line) with w_0 = 0.13, showing the Q-bands spectral shifts and the corresponding change of the absorbance at maximum.

computer-controlled kinetic spectrophotometer, which has been described elsewhere.[47]

Results

Pd(II)TMPy^{4+} Ground-State Spectra. UV−vis spectra of Pd(II)TMPy^{4+} (3.3 μM) in aqueous (pH = 7.0) and in reverse micelles (3% AOT−heptane−H_2O) at different water-to-surfactant molar ratios (w_0 = [H_2O]/[AOT]) are shown in Figure 1. In aqueous solution, the absorption spectrum of Pd(II)TMPy^{4+} showed a Soret band maximum at 417.2 nm (Figure 1) and Q-bands maxima at 525.7 and 553.9 nm (inset, Figure 1). In reverse micellar systems that have a water composition of w_0 > 10.29, all samples showed a similar Soret band red shift (∼3.1 nm) and higher maximum absorption than that observed in aqueous solution. At system compositions below w_0 = 10.29, a Soret band blue shift was observed, increasing with decreasing w_0. In addition, the blue shift was accompanied by the emergence of a new band occurring at ∼390 nm. The maximum absorbance of the new band increased at the expense of the Soret band absorbance. This situation is clearly illustrated in Figure 1 (inset), where a marked spectroscopic Soret band blue shift (∼26 nm) is shown, with a concomitant significant decrease in the maximum absorbance. However, the Q-band observed at λ_{max} = 525.7 nm in aqueous solution was red-shifted to a value of λ_{max} = 534.1 nm in a micellar system. From Figure 1, both wavelengths of the Soret band absorption maxima and the corresponding absorbances were extracted and plotted versus w_0, as shown in Figure 2. As the water-to-surfactant molar ratio increased up to $w_0 \approx 10$, the wavelengths of Soret band absorption maxima underwent a prominent red shift (Figure 2). In micelles of higher water-to-surfactant molar ratio (w_0 > 10), this red shift became practically independent of w_0. Similar trends were observed for the effect of w_0 on the Soret band maximum absorbance (inset, Figure 2).

Figure 3 shows the UV−vis absorption spectra of a neutral aqueous solution of Pd(II)TMPy^{4+} (2 μM) in the absence, and presence, of the oligopeptide K_2YL_2 (116 μM). In the presence of peptide, the spectra revealed an increase of the Soret band absorption at maximum (Figure 3), whereas a decrease of the maximum absorption was observed for the Q-bands (inset, Figure 3). No shifting of either the Soret band or Q-bands was observed.

Zn(II)TMPy^{4+} Ground State and Fluorescence Spectra. UV−vis spectra of a neutral aqueous solution of Zn(II)TMPy^{4+} (6.3 μM) and in reverse micelles (3% AOT−heptane−H_2O) at different w_0 values are shown in Figure 4. In aqueous solution, the Zn(II)TMPy^{4+} ground-state spectra showed a Soret band maximum at λ_{max} = 433.9 nm (Figure 4) and two Q-bands at 562.2 and 604 nm (inset, Figure 4). In reverse micelles, the ground-state absorption spectra of the Zn-porphyrin variant showed characteristics similar to those observed from the Pd-porphyrin variant. The inset of Figure 4 shows the absorbance spectrum of Zn(II)TMPy^{4+} (6.3 μM) in the region of 500−650 nm. As the value of w_0 is increased, all the samples showed a

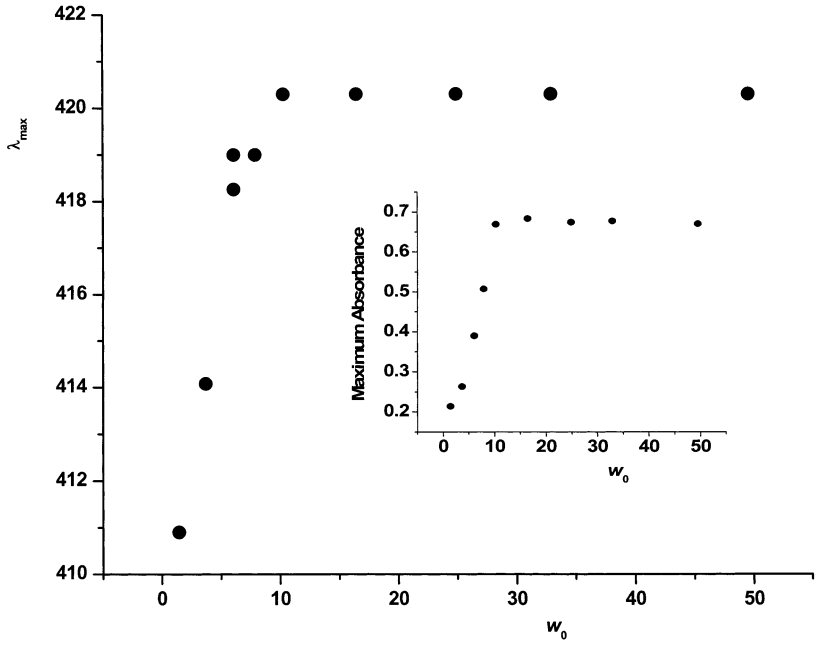

Figure 2. Variation of the wavelengths (λ_{max}) of the Soret band absorption maxima with water micellar content (w_0) for Pd(II)TMPy^{4+} (3.3 μM) in 3% AOT−heptane−H_2O reverse micelles. Inset shows the variation of the absorbance at maximum with w_0.

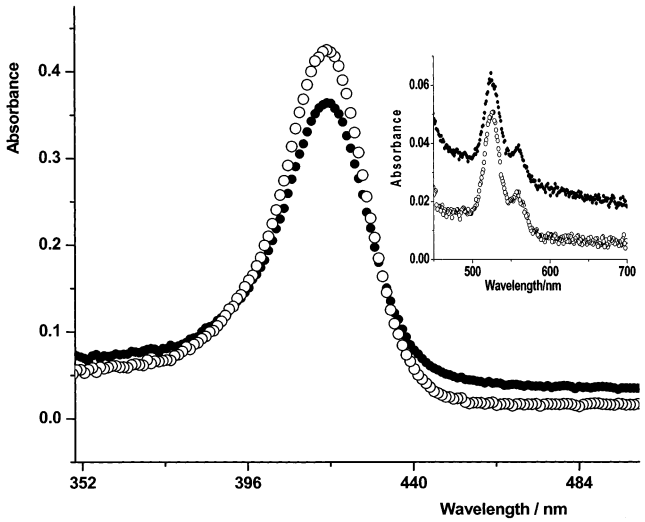

Figure 3. Ground-state absorption spectra of Pd(II)TMPy^{4+} (2 μM) (●) in aqueous (pH = 7.0) solution and (○) in 116 μM K_2YL_2 neutral aqueous solution. Inset shows the ground-state absorption spectra in the range of 450−700 nm.

similar red shift of the Q-bands, relative to the corresponding Q-bands observed in aqueous solution. Variation of the wavelengths (λ_{max}) of the Soret band absorption maxima with w_0 are displayed in Figure 5, where it can be seen that an initial rapid increase of λ_{max} with increasing w_0 is first observed in the low water micellar content range ($w_0 < 10$), followed by a practically w_0-independent regime for higher w_0 values.

The fluorescence spectra of Zn(II)TMPy^{4+} (5.4 μM) was measured in both aqueous (pH = 7.0) solution and in reverse micelles (3% AOT−heptane−H_2O) at different w_0 values (Figure 6). The excitation wavelength used was 563 nm. In aqueous solution, the fluorescence maximum occurred at 631 nm (represented by a solid line in Figure 6). In reverse micellar systems, two different spectral behaviors were noted. In micelles of high water-to-surfactant molar ratio ($w_0 > 8.23$), the fluorescence of all the samples was higher than that in aqueous solution, decreasing with increasing w_0, as shown in Figure 6. In contrast, in micelles of low water composition ($w_0 < 8.23$), the fluorescence was lower than that in aqueous solution and decreased with decreasing w_0. Also, in the range of w_0 investigated ($w_0 = 0.27-48$), all the micellar systems showed a fluorescence emission maximum at $\lambda_{max} = 631$ nm, which is similar to that observed in aqueous solution. The inset in Figure 6 displays the variation of the normalized total fluorescence emission with w_0, where a significant initial increase is observed in the low water micellar content ($w_0 < 8.23$). In micelles of higher water-to-surfactant molar ratio ($w_0 > 8.23$), the normalized fluorescence emission remained practically invariant with w_0.

K_2WL_2 Fluorescence. Fluorescence emission from K_2WL_2 (20 μM) was measured in neutral aqueous solution and in reverse micelles (3% AOT−heptane−H_2O) at different values of w_0. The excitation wavelength used was 230 nm. Plots of the fluorescence spectra obtained are shown in Figure 7, where it can be seen that the maximum fluorescence in aqueous solution occurred at $\lambda_{max} = 354$ nm. As the amount of solubilized water in the micelles is increased, the fluorescence at maximum undergoes a blue shift for all samples. This blue shift is dependent on w_0 and increases as w_0 is decreased. For micelles of low water content ($w_0 < 8.23$), the maximum fluorescence occurred at ~337 nm, whereas for micelles with high w_0 values, the maximum fluorescence emission occurred at ~343 nm. In addition, in both cases, the spectral shift observed for K_2WL_2 in micelles is very significant, compared to that observed in aqueous solution (354 nm). From Figure 7, the fluorescence emission at maximum were extracted and plotted versus w_0 (Figure 8), where it can be seen that the peptide (K_2WL_2) singlet-state fluorescence is considerably quenched upon increasing the water-to-surfactant molar ratio up to $w_0 \approx 10$. In micelles of higher water composition ($w_0 > 8$), K_2WL_2 fluorescence becomes practically independent of w_0. Also shown in Figure 8 (inset) is the variation of the wavelength of maximum fluorescence with w_0. Again, a critical water-to-surfactant molar ratio is $w_0 \approx 10$. Below this critical value, the shift increases as w_0 increases and becomes independent of the water-to-surfactant molar ratio at $w_0 > 10$.

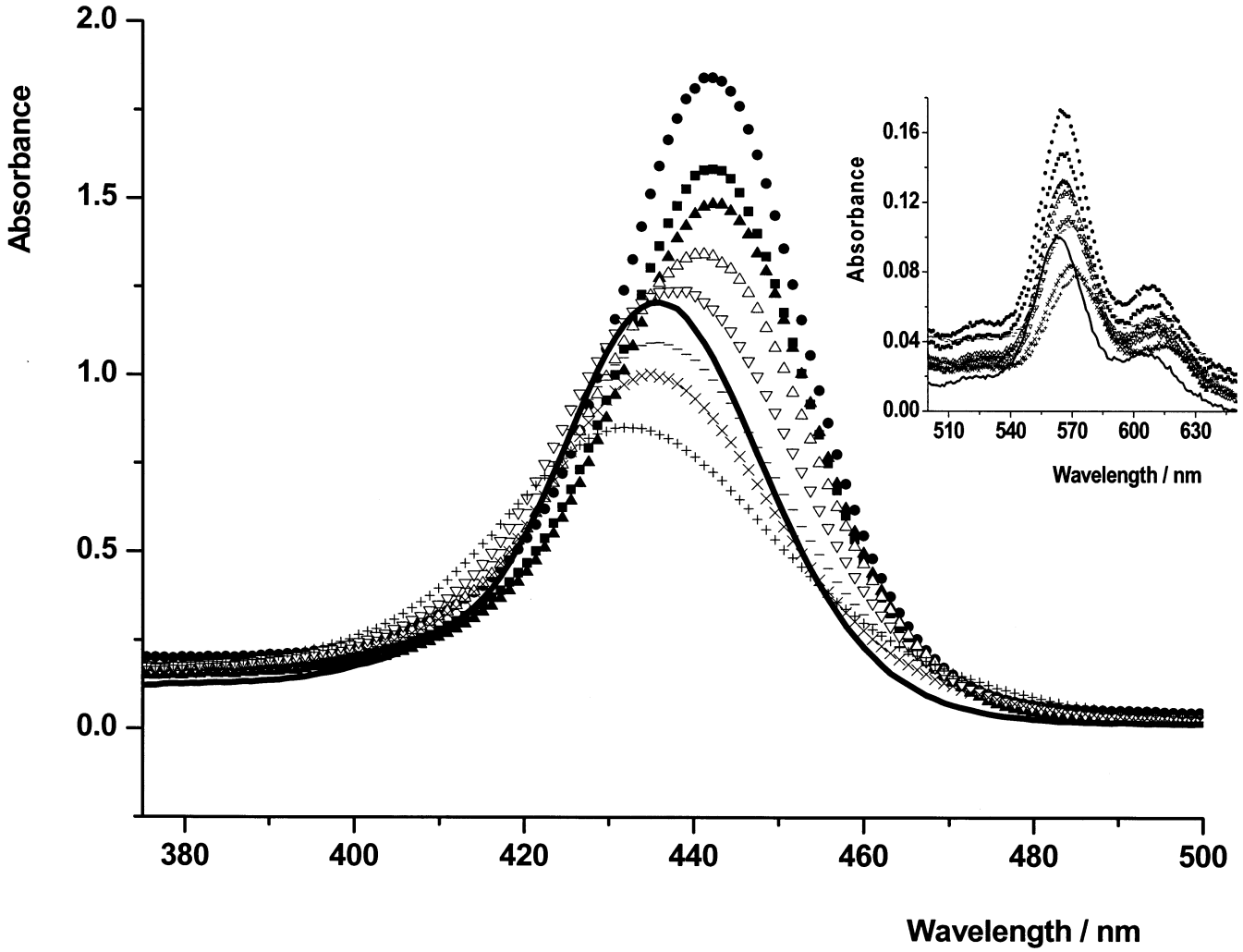

Figure 4. Ground-state absorption spectra of Zn(II)TMPy^{4+} (6.3 μM) in neutral aqueous solution (solid line) and in 3% AOT−heptane−H_2O reverse micelles at the following water-to-surfactant molar ratios, w_0: (●) 49.80, (■) 34.33, (▲) 8.23, (△) 4.11, (▽) 3.29, (−) 2.38, (×) 1.64, and (+) 0.63. Inset shows the ground-state absorption spectra in the range of 500−650 nm.

Pd(II)TMPy^{4+} Triplet State Kinetics. *A. Neutral Aqueous Solutions.* Argon-saturated neutral aqueous solutions of Pd(II)-TMPy^{4+} (2 μM) irradiated with a 6-ns pulse of 532 nm light showed in-pulse formation of a transient absorption with λ_{max} = 460 nm, the decay of which was strictly monoexponential with a decay rate constant of 6.7×10^3 s^{-1} (Figure 9a). This transient was assigned to the porphyrin triplet state (T_1).[9] When the peptide K_2YL_2 (116 μM) was present in the solution, the porphyrin triplet remained monoexponential, as clearly shown in Figure 9b, but with a higher rate constant.

B. In AOT−Heptane−H_2O Reverse Micelle. When an argon-saturated solution of Pd(II)TMPy^{4+} (1.8 μM) in 3% AOT−heptane−H_2O (w_0 = 32.92) was irradiated with a 532-nm laser pulse, a transient absorbing at λ_{max} = 460 nm was observed, the decay of which was strictly monoexponential, as shown in Figure 9c (inset). The rate decay constant of this transient was 3×10^3 s^{-1}. When the peptide K_2YL_2 (480 μM) was present in the micellar solution, the kinetic profile was changed significantly: the decay became faster and markedly nonexponential. This decay was best described by the sum of two exponential terms, as shown by the typical time profile displayed in Figure 9d (inset). For the fast decay component, the evaluated value was 3.64×10^4 s^{-1}, whereas the value for the slow decay component was 4.0×10^3 s^{-1}.

C. Effect of Peptide Concentration on Pd(II)TMPy^{4+} Triplet Kinetics. The experiments previously described were repeated with Pd(II)TMPy^{4+} (1.8 μM) in 3% AOT−heptane−H_2O (w_0 = 8.23) at different K_2YL_2 concentrations. Figure 10 shows the kinetic profile of the porphyrin triplet decay. For the fast decay component (k_f), the evaluated rate constant was found to be independent of the peptide concentration (inset, Figure 10). The mean concentration-independent value was 3.3×10^5 s^{-1}. The slow contribution to the decay profile (k_s) showed a first-order linear dependence (inset, Figure 10) within the peptide concentration range investigated (195−637 μM).

D. Effect of Water-to-Surfactant Ratio on Pd(II)TMPy^{4+} Triplet Kinetics. Laser-pulse excitations at 532 nm of Pd(II)-TMPy^{4+} (2 μM) in 3% AOT−heptane−H_2O were performed at two different w_0 values. The decay profile of the absorbance change at 460 nm of Pd(II)TMPy^{4+} triplet state in the presence of K_2YL_2 (436 μM and 109 μM) at two water-to-surfactant molar ratios (w_0 = 8.23 and 34.58) are shown in Figure 11 (inset). It can be seen that the fast decay component is dependent on w_0. In the micellar system with a low w_0 value (8.23), the evaluated rate constant was $k_f = 2.62 \times 10^5$ s^{-1} (inset, Figure 11a), whereas the corresponding value for the micellar system with w_0 = 34.58 was $k_f = 2.4 \times 10^4$ s^{-1} (inset, Figure 11b). This effect of the water-to-surfactant molar ratio on the overall Pd(II)TMPy^{4+} triplet-state kinetics was investigated at a series

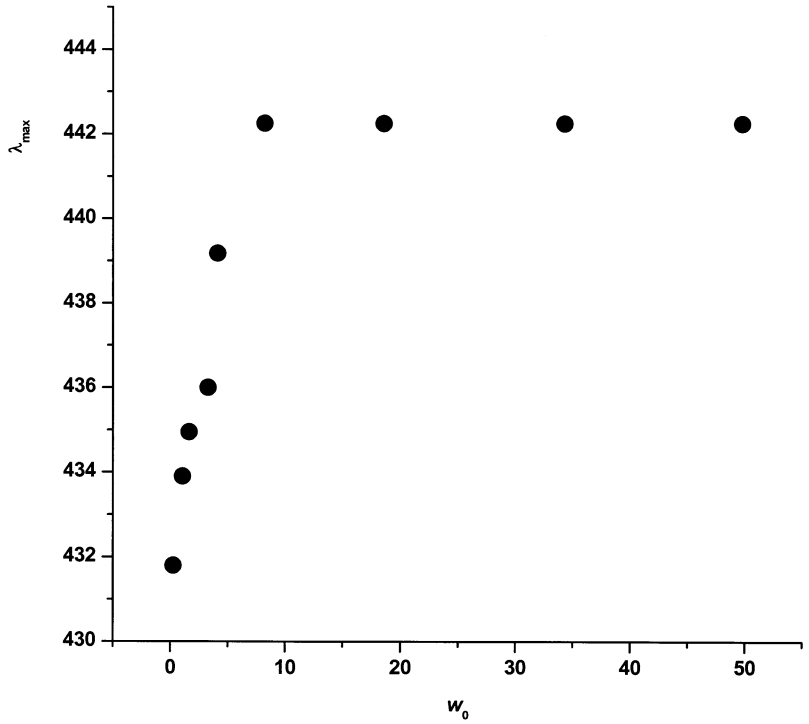

Figure 5. Variation of the wavelength (λ_{max}) of the Soret band absorption maxima with water micellar content (w_0) for Pd(II)TMPy^{4+} (6.3 μM) in 3% AOT−heptane−H_2O reverse micelles.

of w_0 values in the range of 0.13−50 for both peptides (K_2YL_2 and K_2WL_2). A plot of the fast component k_f versus w_0 is shown in Figure 11. The kinetics exhibit an initial rapid decrease for micelles of $w_0 < 5$, followed by a slower one in micelles with a water-to-surfactant molar ratio in the range of $w_0 \approx 5-15$. In micelles with higher water-to-surfactant molar ratios ($w_0 = 15-50$), the decay became slightly independent of w_0.

E. Effect of pH on ZnTMPy^{4+} and PdTMPyP^{4+} Triplet Kinetics. Laser-pulse excitation of ZnTMPyP^{4+} (2.9 μM) in 3% AOT−heptane−H_2O was performed at pH = 7.0. In the absence of the peptide, the porphyrin triplet decay was monoexponential (1.3×10^3 s^{-1}). In the presence of K_2YL_2 (33 μM), the porphyrin triplet state decay remained monoexponential (Figure 12). Repeating the experiment in 3% AOT−heptane−H_2O ($w_0 = 8.32$) in the presence of K_2YL_2 at pH = 10 also revealed a monoexponential decay of the porphyrin triplet state (Figure 12).

Laser-pulse excitation of Pd(II)TMPy^{4+} (1.8 μM) in 3% AOT−heptane−H_2O ($w_0 = 49.38$) in the presence of K_2WL_2 (70 μM) were also performed at three different pH values (2.1, 7.0, and 8.9). Decay profiles of the porphyrin triplet are displayed in Figure 12 (inset), showing no effect of pH on the porphyrin triplet-state decay. A mean value of $k_f \approx 1.68 \times 10^4$ s^{-1} was evaluated.

Discussion

Steady-State Absorption and Emission Spectra. The ground-state absorption behavior of Pd(II)TMPy^{4+} in AOT−heptane−H_2O reverse micelles differ markedly from that in aqueous solution and is strongly dependent on the water-to-surfactant molar ratio w_0 (Figure 1). Clearly, this is an indication that Pd(II)-porphyrin is being solubilized within the micellar water pool as anticipated, because of the highly hydrophilic character of the porphyrin molecule and the coulombic attraction between the negatively charged surfactant headgroups and the tetracationic porphyrin. In particular, a critical water micellar composition was observed at $w_0 \approx 10$ (Figure 2), in accord with the experimental value reported elsewhere.[48] Above this micellar water content and up to $w_0 \approx 50$, the absorption spectra showed that Pd(II)TMPy^{4+} molecule is exposed to a similar aqueous environment, as evidenced by a similar Soret band red shift ($\Delta\lambda = 3.1$ nm; see Figure 2) and a practically constant maximum absorbance (inset, Figure 2). It should be noted that water properties in AOT reverse micelles approach those of bulk water at high micellar water content. This appearance of free water is usually observed in the range of $w_0 \approx 10-15$.[48] In the large w_0 range (up to ∼50) investigated in this work, the spectral characteristics of Pd(II)TMPy^{4+} in reverse micelles never approached those observed in aqueous solution, indicating that porphyrin molecules are preferentially solubilized in the micelle interfacial region and not in the bulklike water inner core of the micelle. In micelles that have a water composition less than $w_0 \approx 10$, the main features of the results shown in Figures 1 and 2 may suggest that the Pd(II)-porphyrin molecule is being exposed to a different aqueous environment within the water pool, depending on the amount of water solubilized in the micellar core. Investigations have generally confirmed[49,50] the existence of distinct populations of water molecules in reverse micelles, namely surfactant "bound" water, trapped (interfacial) water, and "bulk" water, the latter of which emerges as the surfactant headgroups, and counterions become saturated as the micellar water content increases. At low micelle water compositions, the first type of water ("bound" water) predominates, with the consequence that solvated solubilized molecules experience a rigidly structured aqueous environment of low polarizability and high microviscosity. These populations are frequently described as being confined in physically defined layers of fixed thickness. Therefore, the observed w_0 dependency of the Soret band shift in micelles that have a water composition of $w_0 < 10$ is probably indicating that the porphyrin molecule is being solubilized in different layers of water molecules, depending on the value of w_0. The first water layer is being strongly bound

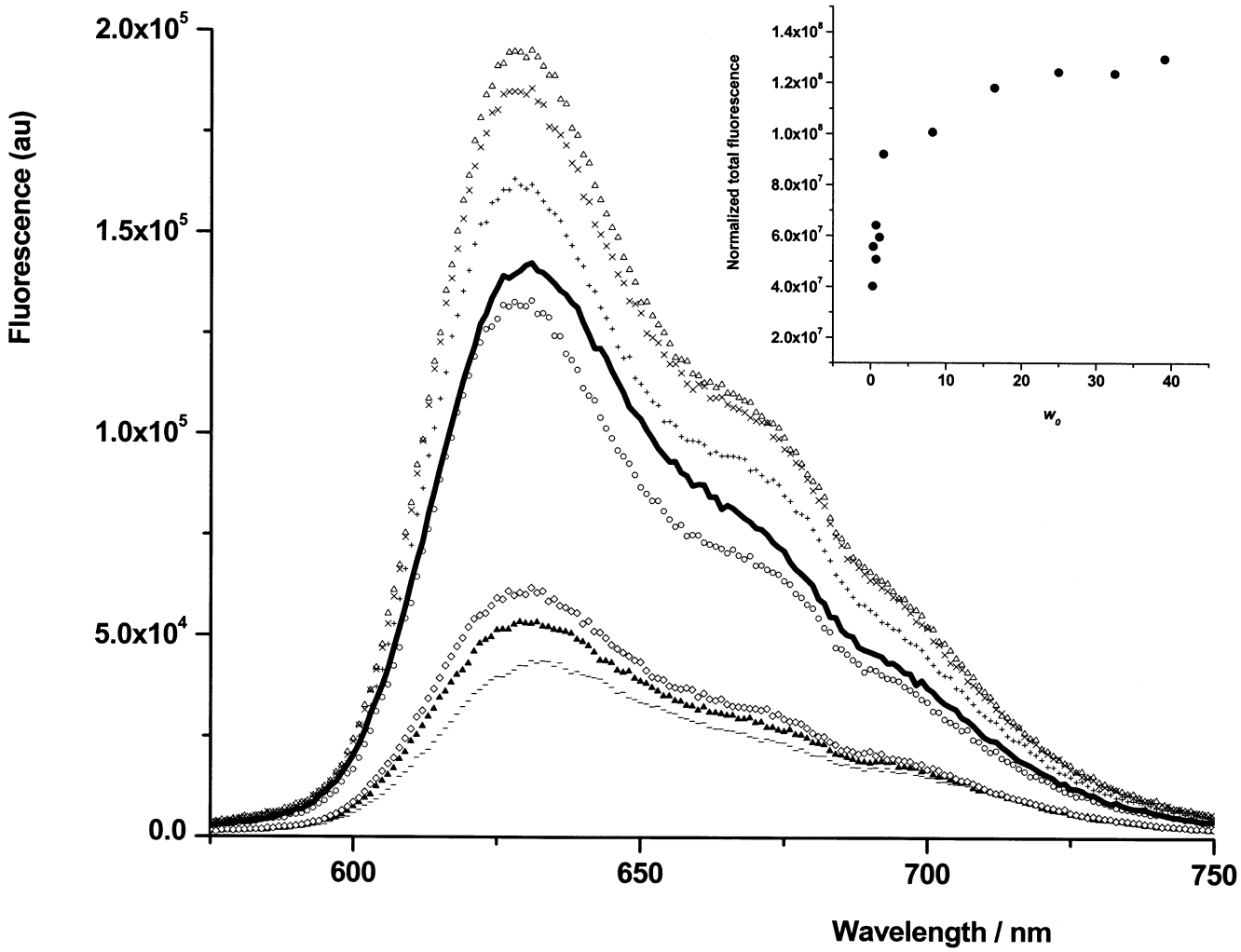

Figure 6. Fluorescence spectra of Zn(II)TMPy^{4+} (5.4 μM) in aqueous (pH = 7.0) solution (solid line) and in 3% AOT−heptane−H_2O reverse micelles at the following water-to-surfactant molar ratios, w_0: (−) 0.27, (▲) 0.72, (◇) 1.63, (○) 3.48, (△) 8.23, (×) 32.55, and (+) 48 (λ_{exc} = 563 nm). Inset shows the variation of the normalized fluorescence emission with w_0.

to the surfactant headgroups, whereas the subsequent water layers become less bound as hydration increases. Ultimately, the water type in each layer becomes progressively more bulklike.

The exact location in the micelle at which solubilization occurs reflects the type and strength of interactions that are occurring between the surfactant and the solubilizate.[51] Thus, one may invoke electrostatic interactions between the negatively charged surfactant headgroups and the tetracationic porphyrin molecules as the main driving force behind the solubilization process. The strength of this coulombic interaction is determined by the separation distance between the surfactant headgroups and the porphyrin molecule. Increasing the amount of solubilized water will induce an increase of the mean distance between the interacting species and, consequently, a decrease of their mutual attraction. For instance, at a very low micellar water content (w_0 = 0.13, i.e., one water molecule for approximately seven surfactant molecules), relatively few water molecules are adsorbed at the micelle interface, thereby allowing for a strong electrostatic interaction between the porphyrin molecules and the surfactant headgroups and a plausible ion-pair formation. This is reflected by the observed significant Soret band blue shift (inset, Figure 1). As more water is added, successive thin layers of water molecules start to form, thereby increasing the separation distance between the interacting species and, consequently, their mutual coulombic attraction. This is reflected by the observed splitting of the Soret band (inset, Figure 1). Thus, the aforementioned results seem to indicate that electrostatic interactions between the tetracationic porphyrin molecules and the surfactant anionic polar headgroups play a key role in the specific localization of the porphyrin molecule in reverse micelles.

The ground-state spectra of Zn(II)TMPy^{4+} in reverse micelles (Figures 4 and 5) showed characteristics similar to those observed with Pd(II)TMPy^{4+} porphyrin, namely (i) there is a critical micellar water composition of $w_0 \approx 10$; (ii) a similar porphyrin aqueous microenvironment exists for micellar water compositions of $w_0 > 10$; (iii) different sites of solubilization of the porphyrin molecule are observed for micelle water compositions of $w_0 < 10$; and (iv) the porphyrin molecule is preferentially solubilized in the micellar periphery and not in the bulklike inner micellar water core. However, it is interesting to note a fundamental difference between the absorption spectra of Zn(II)TMPy^{4+} and Pd(II)TMPy^{4+}. For Pd(II)TMPy^{4+} and below the critical water micellar water composition ($w_0 < 10$), a splitting of the Soret band occurred as the value of w_0 is decreased, accompanied by the emergence of a new absorption band at ~390 nm. This Soret band splitting is not observed for the Zn(II)-porphyrin variant. This difference may indicate a weaker interaction between AOT polar headgroups and Zn(II)-TMPy^{4+}, compared to the corresponding interaction with Pd-(II)TMPy^{4+}.

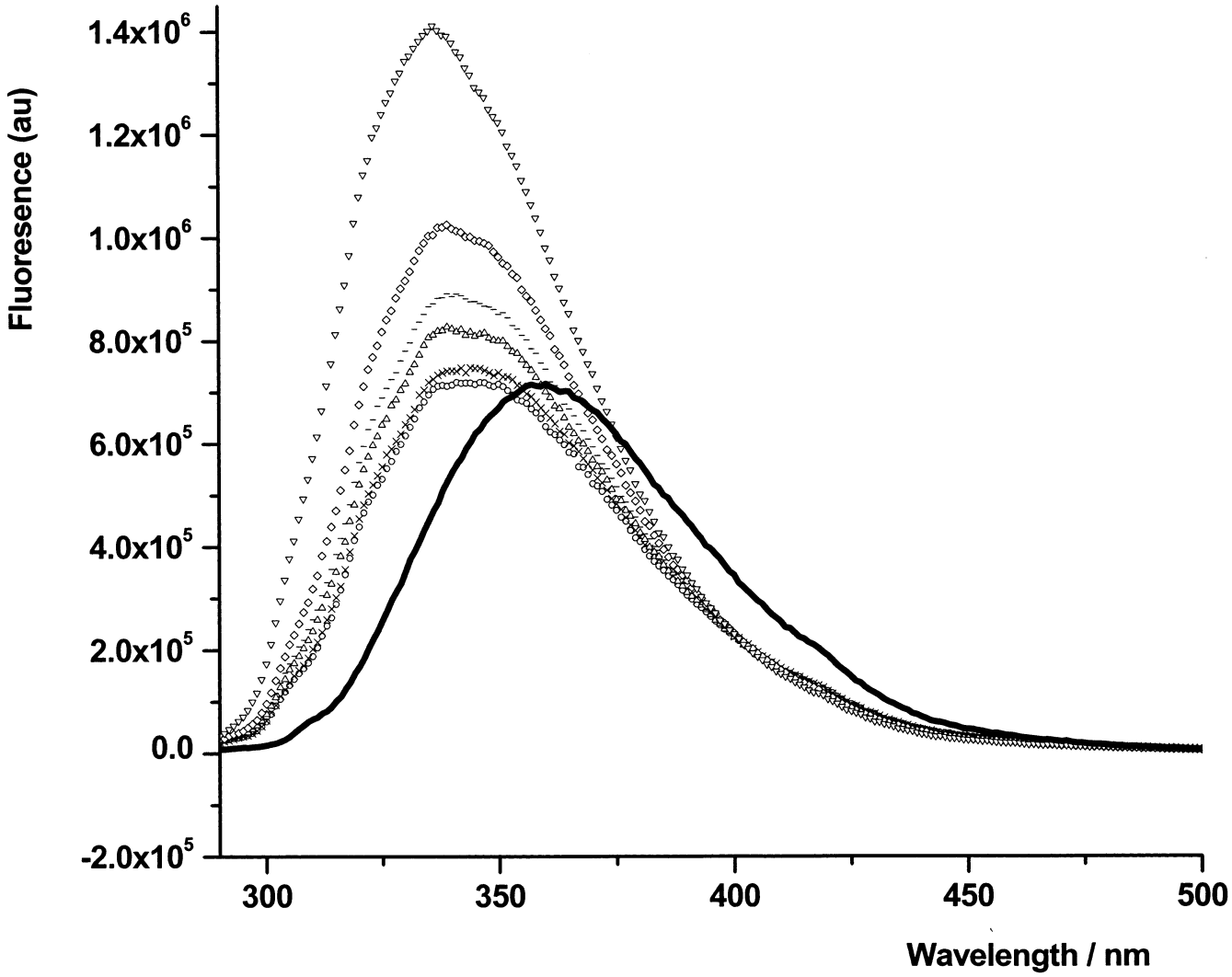

Figure 7. Fluorescence spectra of K_2WL_2 (20 μM) in aqueous (pH = 7.0) solution (solid line) and in 3% AOT−heptane−H_2O reverse micelles at the following water-to-surfactant molar ratios, w_0: (▽) 1.40, (◇) 4.12, (−) 6.25, (△) 8.23, (×) 24.70, and (○) 41.16 (λ_{exc} = 563 nm).

ZnTMPyP^{4+} fluorescence spectra also revealed a critical micellar water composition of $w_0 \approx 10$. Below the critical micellar water, the w_0-dependent fluorescence enhancement (Figure 6) is also reflecting different sites of solubilization of the porphyrin molecule within the different water layers, corresponding to different w_0 values. Above $w_0 \approx 10$, the porphyrin fluorescence intensity is practically constant (inset, Figure 6), reflecting a similar solubilizate aqueous microenvironment. Clearly, these results are in good agreement with those derived from Zn(II)TMPy^{4+}ground-state absorption behavior.

The fluorescence spectrum of K_2WL_2 incorporated in AOT−heptane−H_2O reverse micelles differs from that observed in aqueous solution (Figure 7), again revealing a critical water micellar composition at $w_0 \approx 10$ (Figure 8). Furthermore, it is relevant to mention that the fluorescence of K_2WL_2 in aqueous solution is different from that of the monomeric tryptophan species in water. In aqueous solution, the fluorescence spectrum usually consists of a single, unstructured band with a maximum at ~348 nm.[52] The fact that the tryptophan fluorescence in K_2YL_2 is red-shifted (λ_{max} = 354 nm) may suggest that the tryptophan environment is affected when it is incorporated in the middle of the pentapeptide backbone (L_2WK_2). The quenching of the fluorescence of amino acid residues (tyrosine (Y), tryptophan (W)) in peptides has been the subject of much discussion, and different mechanisms have been proposed which focus on the role of the local environment of the fluorescent moiety in a protein or peptide.[53] In the low micelle composition range ($w_0 < 10$), the peptide maximum fluorescence emission and the wavelength at emission maximum (λ_{max}) are very sensitive to the peptide microenvironment (Figure 8), suggesting different solubilization sites for the oligopeptide molecule, depending on w_0. On the other hand, in micelles with higher water content ($10 < w_0 < 50$), the maximum fluorescence emission and λ_{max} remain practically constant, reflecting a similar aqueous microenvironment for the oligopeptide. This finding is in accord with ground-state spectroscopic measurements, using the porphyrin molecules (Zn(II)TMPyP^{4+} and Pd(II)TMPy^{4+}) as extrinsic probes. Furthermore, the fluorescence behavior of K_2WL_2 in reverse micelles never approached the corresponding behavior in aqueous solution, suggesting that the oligopeptide is preferentially solubilized in the micellar interface and is not shifted toward the bulklike central pool of the reverse micelle. Such conclusions are also in agreement with those derived from (Pd(II)TMPy^{4+} and Zn(II)TMPy^{4+}) ground-state absorption spectra and from (Zn(II)TMPy^{4+}) singlet-state fluorescence spectra characteristics.

Transient Kinetics Studies. The hypothesis behind this research work was that, in AOT−heptane−H_2O reverse micelles, tetracationic water-soluble porphyrins (Pd(II)TMPy^{4+} and Zn(II)TMPy^{4+}) and oligopeptides, such as those employed

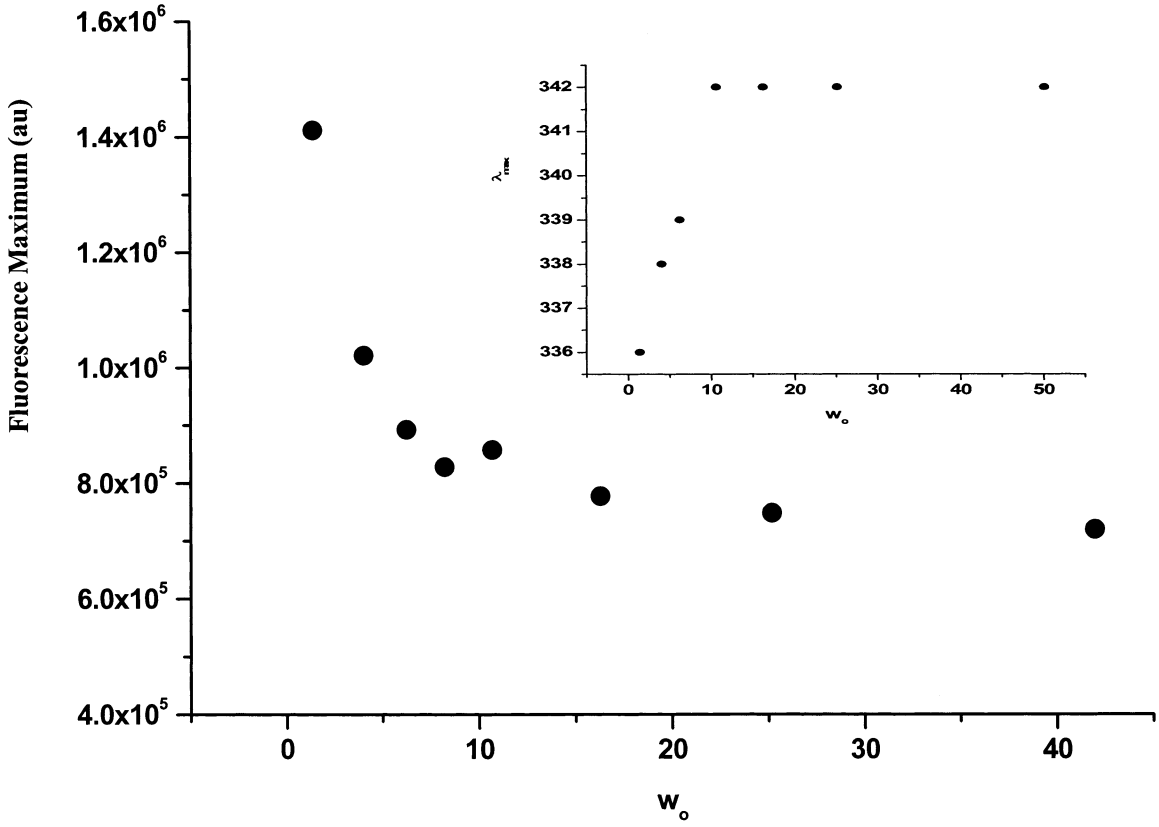

Figure 8. Variation of the fluorescence intensity at λ_{max} with w_0 for K_2WL_2 (20 μM) in 3% AOT−heptane−H_2O reverse micelles. Inset shows the variation of the fluorescence emission maximum wavelength with w_0.

herein (K_2WL_2 and K_2YL_2), would be associated with the micelles and, therefore, would be confined within a same volume fragment. The electrostatic interactions between the tetracationic and the anionic entities (surfactant headgroups) could lead to a solubilization of porphyrin molecules in the inner micellar interface. Also, the appropriate choice of oligopeptides that have a relatively very hydrophobic amino acid residue (L) and a very hydrophilic amino acid residue (K) would favor an oligopeptide solubilization within the micellar interface. Therefore, such a model would then place the oxidizable portion of the target residue (Y and W) in proximity to the porphyrin triplet state, T_1. Evidence for a restricted solubilization of both porphyrin and oligopeptide in the micelle interface region is provided from the ground-state absorption spectra of Pd(II)TMPy^{4+} and Zn(II)TMPy^{4+} and from the emission spectra of Zn(II)TMPy^{4+} and K_2YL_2, confirming the aforementioned hypothesis.

In neutral aqueous solutions (Figure 9a), the triplet-state decay of Pd(II)TMPyP^{4+} (2 μM) showed single-exponential kinetics ($k = 6.7 \times 10^3$ s^{-1}). Upon the addition of the oligopeptide K_2YL_2 (116 μM) to the solution, the T_1 porphyrin state decayed, according to a single exponential but with a higher rate constant (Figure 9b). The fact that the triplet decay is faster in the presence of peptide is probably a consequence of a bimolecular quenching of the porphyrin triplet state by the oligopeptide. In fact, this peptide−porphyrin triplet-state interaction in aqueous solution was also reflected in the UV−vis absorption spectra (Figure 3). Furthermore, the porphyrin triplet-state decay remains monoexponential, indicating no evidence for electron-transfer reaction between the target (Y) and the porphyrin triplet state, which is similar to that observed in self-assembled complexes of oligopeptides with metalloporphyrins.[9,10] This may be understood through the fact that, in aqueous solution, the tyrosine moiety is, on average, located at a relatively large distance from the porphyrin molecule for electron transfer to occur. In AOT−heptane−H_2O reverse micelles, a different behavior was observed (inset, Figure 9). In the absence of peptide (inset, Figure 9c), the porphyrin triplet-state decay is strictly monoexponential ($\sim 3 \times 10^3$ s^{-1}). The inclusion of K_2YL_2 into the micelle system converts what is initially a single-exponential triplet-state decay into a biexponential (best fitted with the sum of two exponentials) decay, which suggests that the peptide is seriously perturbing the triplet state of the Pd-porphyrin (inset, Figure 9d).

At this juncture, it is relevant to note the interesting similarity between the observed kinetics of the porphyrin triplet-state decay in AOT reverse micelles on one hand, and that in self-assembled complexes of oligopeptides with metalloporphyrin in neutral homogeneous solution on the other.[9] In self-assembled complexes, the target (Y and W) moieties are brought in proximity of the porphyrin molecule, via electrostatic interaction, setting up the possibility for the observed electron transfer from the target-peptide molecule to the porphyrin triplet state T_1.[9] This same situation may be invoked to explain the similar kinetic behavior observed in AOT reverse micelles. Steady-state measurements showed strong evidence for a restricted solubilization of porphyrin and oligopeptide molecules the oil−water micellar interface. The porphyrin is being solubilized in the water pool, confined to the water−AOT molecular interface, and surrounded by the adsorbed or trapped water molecules (depending on w_0). On the other hand, the oligopeptide is restricted to the oil−micelle interface with the target moiety (W and Y) being solubilized at the oil−AOT molecular interface. Consequently, this will bring the target moiety in proximity to the porphyrin molecule, setting up the possibility for a plausible intramicellar electron transfer from the target molecule to the porphyrin T_1 state. Thus, at this stage, one may

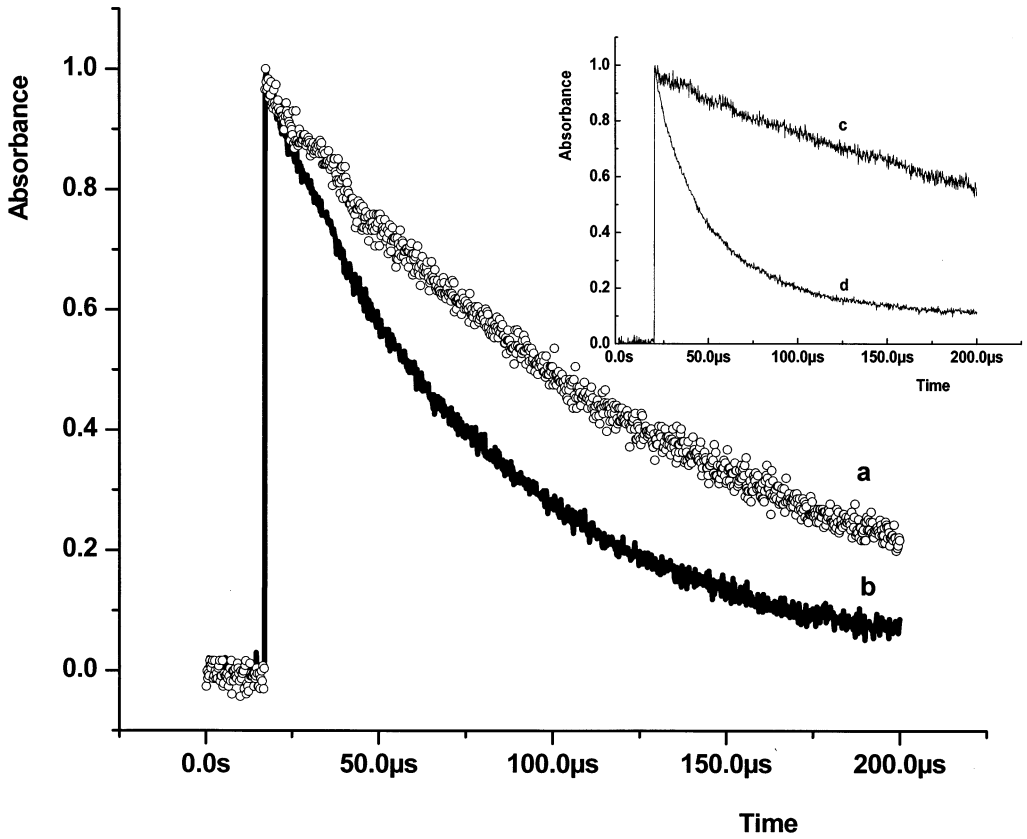

Figure 9. Normalized decays of the absorbance change at 460 nm following pulsed 532-nm excitation of an argon-saturated neutral aqueous solution of Pd(II)TMPy^{4+} (2 μM) in the (a) absence and (b) presence of K_2YL_2 (116 μM). Inset shows similar normalized decays of the absorbance change of an argon-saturated neutral aqueous solution of Pd(II)TMPy^{4+} (1.8 μM) in 3% AOT−heptane−H_2O ($w_0 = 32.40$) in the (c) absence and (d) presence of K_2YL_2 (480 μM).

suggest that the change in the kinetics of the porphyrin triplet state in AOT reverse micelles (biexponential decay), compared to that observed in homogeneous aqueous solution (single-exponential decay), involve an electron-transfer reaction between the reacting species.

Further evidence for the aforementioned conclusion was sought from the investigation of the effect of peptide concentration on the porphyrin triplet-state decay (Figure 10). Interestingly, the evaluated rate constants for the fast decay component (k_f) and the slower decay componenet (k_s) were found to be independent of the peptide concentration ($k_s = 3.3 \times 10^5$ s^{-1}) and dependent on the first-order concentration, respectively (inset, Figure 10). Again, this kinetic behavior was also observed in self-assembled oligopeptide−metalloporphyrin complexes, whereas the fast component (which was independent of peptide concentration) of the porphyrin T_1 state decay was associated with an intracomplex electron transfer and the slower component (which was dependent on peptide concentration) was associated with the diffuse formation of an encounter complex between the free peptide (bulk phase) and the porphyrin molecule, followed by an electron transfer. This similarity in the mode of deactivation of the T_1 state in both self-assembled complexes and AOT reverse micelles makes the assumption that the porphyrin triplet-state decay in AOT micelles is due to an electron-transfer event more attractive.

Having shown that the rate constant of the T_1 fast decay component is independent of peptide concentration, it is appropriate to investigate the effect of w_0 on the porphyrin T_1-state quenching process. In general, the rate constant for electron transfer decreases exponentially with the donor−acceptor separation distance.[10] The size of the water pool (and, therefore, the reverse micellar radius) is directly related to w_0. As seen in Figure 11, the fast component k_f showed a clear dependence on the micellar radius, as expected for an electron-transfer rate constant. A critical micelle water composition was observed at $w_0 \approx 10$, in accord with steady-state measurements.

The comparison made thus far between the quenching of the T_1 state in the homogeneous aqueous system and that in the microheterogeneous system should be considered with caution. Fundamental differences exist between these two systems, which may be relevant to the mechanism of the triplet-state deactivation process. In reverse micelles, one must consider the distribution law for guest molecules among the aggregates. Furthermore, reverse micelles are in dynamic equilibrium and micellar exchange processes of solubilizates occur.[48] Particularly, the first investigations in AOT systems demonstrated that such an exchange of material between reverse micelles was facile.[54] In subsequent independent studies,[55−58] the micellar exchange rate constant (k_e) was evaluated to be $\sim 10^7$ M^{-1} s^{-1} in AOT reverse micelles. Strong evidence was shown for a micellar exchange via a mechanism involving transient fusion[48] of two micelles to form a short-lived "transient droplet". During the lifetime of this transient (microsecond-range) solubilized species, together with water and surfactant, can randomly redistribute by translational diffusion. Subsequently, the transient splits into two micelles, which are not necessarily identical to the original micelles.[59]

Using a sensitizer in its photoexcited state (singlet or triplet), various types of kinetics were observed.[54,60] In reverse micelles where the probe is not associated with the micelle, the excited state decays monoexponentially.[61,62] In micellar systems where the probe is associated with the micelle, a two-component decay

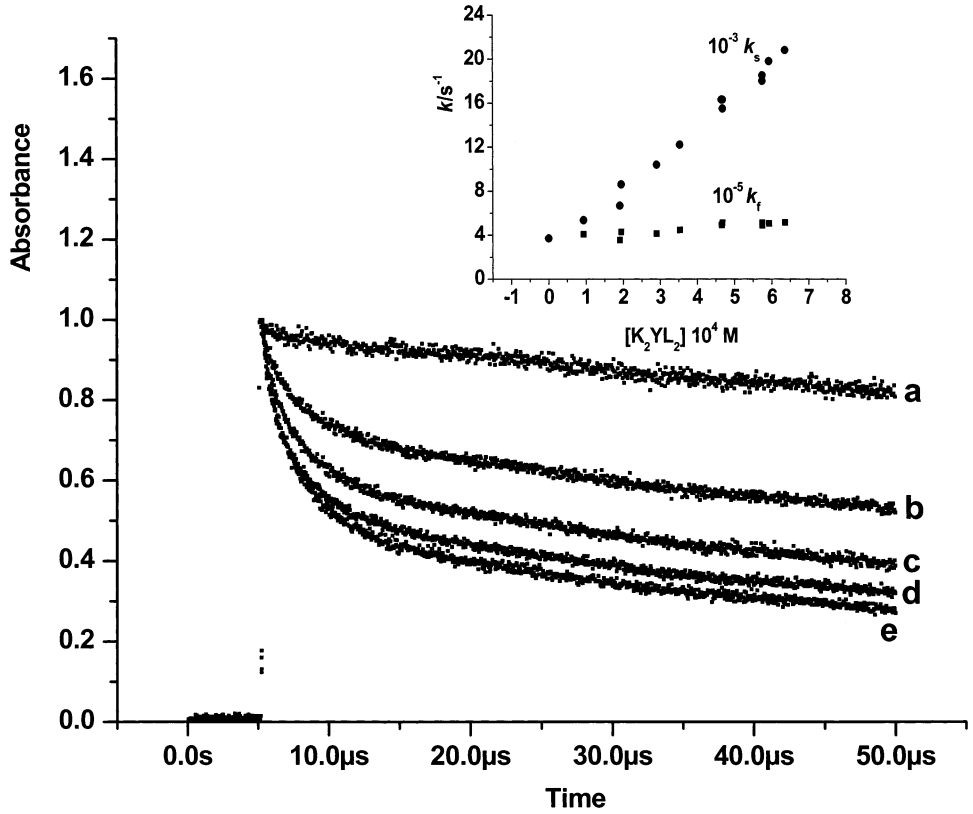

Figure 10. Normalized decays of the absorbance change at 460 nm following pulsed 532-nm excitation of an argon-saturated neutral solution of Pd(II)TMPy^{4+} (1.8 μM) in 3% AOT−heptane−H_2O (w_0 = 8.23) at different K_2YL_2 concentrations: (a) 0 μM, (b) 195 μM, (c) 354 μM, (d) 469 μM, and (e) 575 μM. Inset shows the variation of (■) the fast component k_f and (●) the slow component k_s of Pd(II)TMPy^{4+} (1.8 μM) triplet decay in argon-saturated neutral solutions in 3% AOT−heptane−H_2O (w_0 = 8.23) with K_2YL_2 concentration.

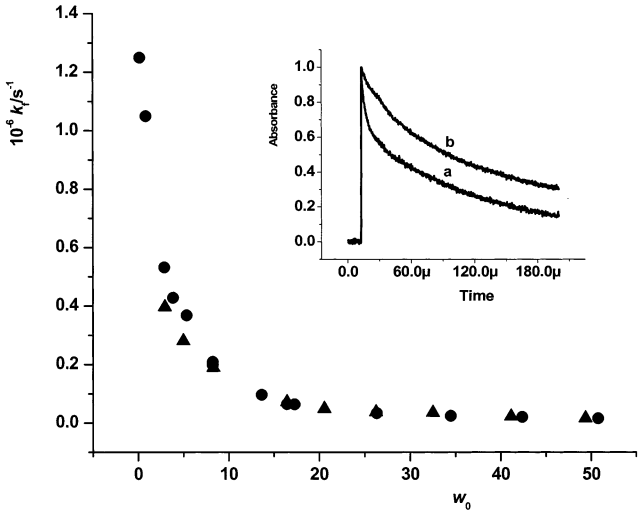

Figure 11. Variation of the fast-component (k_f) decay rate constant of PdTMPy^{4+} (2 μM) triplet decay in argon-saturated neutral solutions in 3% AOT−heptane−H_2O at different water−surfactant molar ratios w_0 in the presence of (●) 254 μM K_2YL_2 and (▲) 275 μM K_2WL_2. Inset shows normalized decays of the absorbance change at 460 nm following pulsed 532-nm excitation of an argon-saturated neutral solution of Pd(II)TMPy^{4+} (1.8 μM) in 3% AOT−heptane−H_2O at two different water-to-surfactant molar ratios: (a) w_0 = 8.32 and (b) w_0 = 32.93.

is observed. The fast decay is due to intramicellar quenching and is characterized by a quenching rate constant k_q. When the lifetime of the sensitizer in its excited state is shorter than the time required for intermicellar exchange, the slow transient component is due to the decay of the sensitizer in its excited state, when located in micelles containing no quenchers.[63,64] For such a case, the long time decay is independent of the quencher concentration. For the case in which the lifetime of the sensitizer is longer than the time scale for micellar exchange,[57,65] the slowest component decay is due to the decay of the sensitizer and to quenching that occurs when a quencher is exchanged between one droplet and another. In such a case, the slope of the slow component decay increases as the quencher concentration increases. Accordingly, it seems appropriate to suggest that the fast-component decay is indeed associated with an intramicellar electron-transfer process from the target moiety (Y and W) to the porphyrin triplet state. This electron-transfer event occurs during the lifetime of a discrete micelle between the oxidizable moiety and the photoexcited porphyrin molecule, both being solubilized at the water−micelle interface. Two interesting observations support this conclusion. First, k_f was found to be concentration independent (inset, Figure 10), as expected for an electron-transfer rate constant. Second, k_f was found to be strongly dependent on the amount of water in the micelles (Figure 11), i.e., on the separation distance between the reactive species. However, for the aforementioned suggestion to be valid, the lifetime of a discrete micelle should be sufficiently long for the electron-transfer event to occur. This lifetime (τ_M) is dependent on the micelle concentration ([M]) of the system and may be evaluated by the following expression:

$$\tau_M = (k_{ex}[M])^{-1} \quad (2)$$

where k_{ex} is the micellar exchange rate constant. [M] is related to the water-to-surfactant molar ratio, w_0. Thus, at w_0 = 4.16 (0.5% water, v/v), the micelle concentration is [M] = 8.7 × 10^{-4} M.[66] Taking a typical k_{ex} value of 10^6 M^{-1} s^{-1}, the micelle lifetime would be τ_M = 1.15 ms. At this micellar water

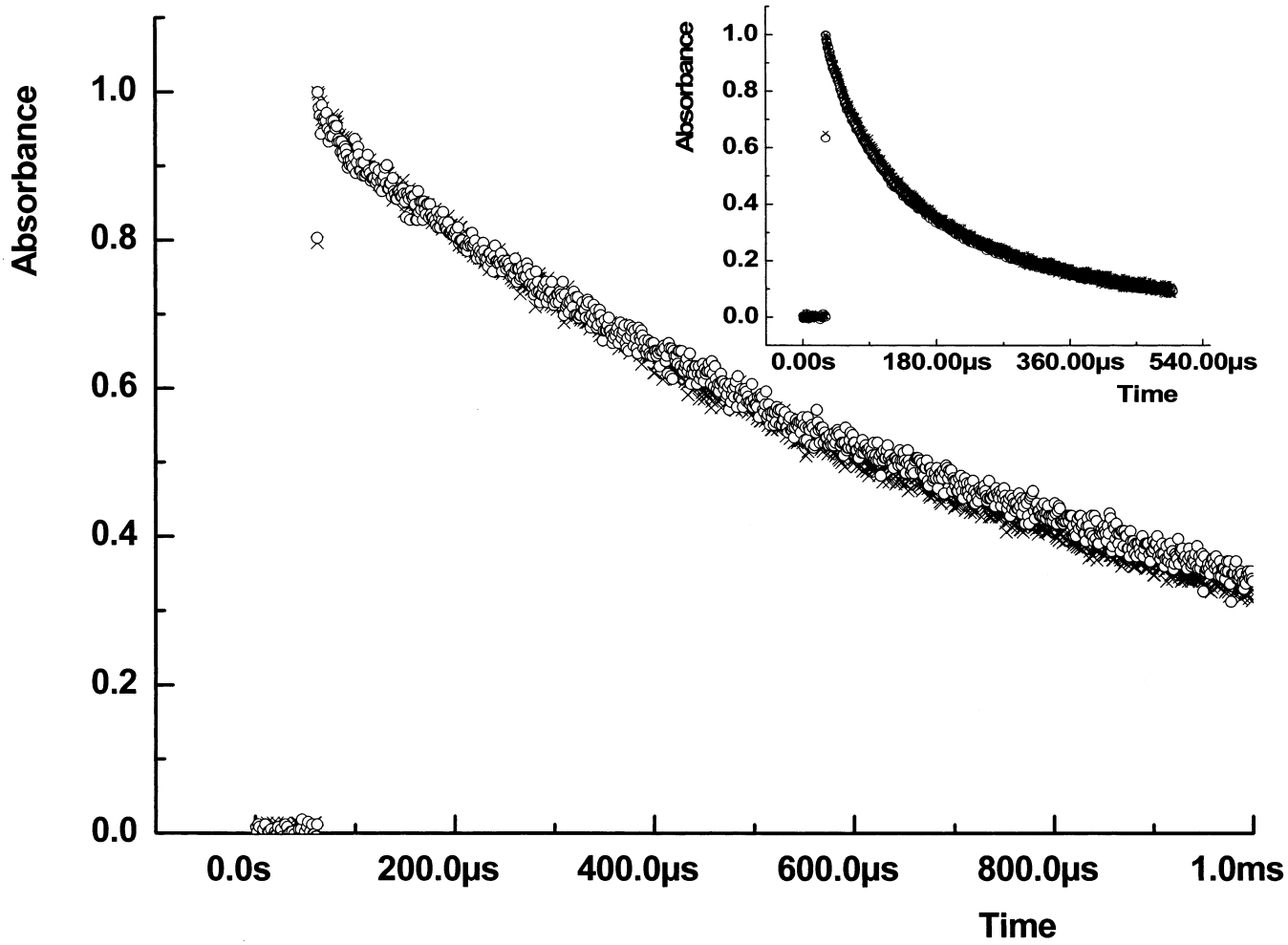

Figure 12. Normalized decays of the absorbance change at 480 nm following pulsed 532-nm excitation of an argon-saturated solution of Zn(II)-TMPy^{4+} (2.9 μM) in the presence of K_2YL_2 (33 μM) at (○) pH = 7.0 and (×) pH = 10.0. Inset shows normalized time profiles of the absorbance changes at 460 nm following pulsed 532-nm excitation of an argon-saturated solution of Pd(II)TMPy^{4+} (1.8 μM) in 3% AOT−heptane−H_2O (w_0 = 50) in the presence of K_2WL_2 (70 μM) at different pH: (○) 2.1, (×) 7.0, and (+) 8.9.

composition, the fast-component rate constant of the decay was found to be $k_f = 4.3 \times 10^5$ s^{-1} ($1/k_f = 2.3$ μs). A similar calculation at $w_0 = 8.32$ (1% water, v/v), where the overall concentration of reverse micelle is 2.16×10^{-4} M, yields a micelle lifetime equal to 4.6 ms. The measured fast-component decay at this composition was $k_f = 2 \times 10^5$ s^{-1} ($1/k_f = 50$ μs). Finally, in micelles having $w_0 \approx 50$ (6% water, v/v), the overall micelle concentration is relatively low (6×10^{-6} M), yielding a micelle lifetime equal to 6 ms. The corresponding measured fast-component decay rate constant is $k_f = 1.6 \times 10^4$ s^{-1} ($1/k_f = 62.5$ μs). As illustrated from these calculations, the lifetime of a discrete micelle for a given micellar water composition is sufficiently long for the fast component of the quenching process to occur.

Having shown that the fast-component decay is probably associated with an electron-transfer event, it is appropriate to turn to the slow-component decay. This decay (k_s) was found to be dependent on the quencher concentration. As previously mentioned,[57,65] such kinetic behavior occurs when the lifetime of the photoexcited state is longer than the time of micelle exchange. In this investigation and in the absence of peptide (Figure 10a), the measured lifetime of the porphyrin triplet state was found to be on the order of milliseconds ($\tau_T \approx 0.330$ ms). Experimental data for AOT are consistent with a lifetime of the transient droplet in the microsecond time range.[48] The lifetime of the porphyrin triplet state is, therefore, sufficiently long enough for the micelle contents to randomize effectively by diffusion, resulting in the quenching of the porphyrin triplet state via the slow deactivation process (k_s).

Additional investigation of this electron-transfer reaction was done with the Zn(II) variant in place of the Pd(II) variant as the putative electron acceptor. In the in the absence of K_2YL_2 at pH = 7.0, the triplet-state decay profile of Zn(II)TMPy^{4+} showed single-exponential kinetics with a rate constant $k = 0.92 \times 10^3$ s^{-1}. In the presence of K_2YL_2 (33 μM), the T_1 decay remains single-exponential with a somewhat higher rate constant, $k = 1.9 \times 10^3$ s^{-1} (Figure 12). This increase in the rate constant may be due to the quenching of the T_1 state during micellar exchange. The absence of electron transfer between Zn(II)TMPy^{4+} and the target moiety of the oligopeptide is simply reflecting a thermodynamically unfavorable situation for the electron transfer to occur. In aqueous homogeneous solution and at pH = 7.0, the reduction potential of the tyrosine radical cation is 0.93 V and that of the T_1 state of Zn(II)TMPy^{4+} is quoted to be 0.78 V. Therefore, $\Delta E^0 = 0.78$ V− 0.93 V = −0.15 V; hence, the electron-transfer process for tyrosyl is energetically unfavorable. Interestingly, the reduction potential of the tyrosine system can be manipulated by changing the pH of the system in aqueous solution. Thus, at pH = 10.0, the reduction potential of tyrosine is shifted to 0.72 V, thereby putting the driving force for the electron-transfer process at $\Delta E^0 = 0.78$ V − 0.72 V = 0.06 V, i.e., in the thermodynamically

favorable region. Nevertheless, at this pH, the $ZnTMPyP^{4+}$ porphyrin triplet-state decay profile in reverse micelles remained single-exponential (Figure 12). At this same pH, in self-assembled oligopeptide−porphyrin complexes aqueous homogeneous solutions, the $Zn(II)TMPyP^{4+}$ decay profile was double exponential,[9] confirming that the intracomplex quenching can occur when the driving force for electron transfer is favorable.

In aqueous homogeneous solutions, the redox potentials for one-electron oxidation of tyrosine and tryptophan indicated that the target amino acids (Y and W) are not affected by the peptide environment. In self-assembled peptide−metalloporphyrin complexes, the target residues (Y and W) are also probably experiencing an aqueous environment similar to the environment within the peptide in aqueous solutions, because of their terminal position within the peptide backbone (E_4Y and E_4W). On the contrary, in AOT−heptane−H_2O systems, the situation seems to be different. Ground-state absorption and single-state fluorescence measurements showed a strong evidence that both porphyrins and oligopeptides are preferentially solubilized within the micellar oil−water region. Therefore, the actual values of the reduction potentials E^0 in AOT reverse micelles are probably different from the corresponding potentials in bulk aqueous solutions; thus, the estimation of the driving force ΔE^0 in AOT from E^0 values determined in aqueous solutions is probably misleading. Another interesting issue involves the actual meaning of the concept of pH in reverse micelles. The pH used in the aforementioned calculation of the driving force ΔE^0 in reverse micelles refers to the pH of the injection stock solution with which the water pool of reverse micelle is created (pH_{st}). Evidence has been shown that the pH in the water pool (pH_{wp}) is different from pH_{st}.[67] El Seoud[68] computed pH_b (bound water) and pH_f (free water) for various pH_{wp} and w_0 values. The results showed that the pH values at the micellar periphery (pH_b) and at the center part of the pool (pH_f), as a function of pH_{wp}, differ according to the value of w_0. For a small pool ($w_0 = 10$), this difference is ~0.5 pH units ($pH_f > pH_b$), whereas in a larger water pool ($w_0 = 40$), the difference is relatively higher (~1.5 pH units). As a result, one cannot calculate the driving force for the electron transfer reaction in AOT reverse micelles by simply using the E^0−pH relation, measured in homogeneous aqueous solutions.

Finally, to investigate this pH effect on the electron-transfer reaction further, the decay of the $Pd(II)TMPyP^{4+}$ triplet state T_1 in AOT reverse micelles was also investigated at three different pH (inset, Figure 12). Interestingly, the decay was found to be pH-independent. This finding contrasts with the kinetic behavior observed in self-assembled oligopeptide (E_4Y and E_4W)−porphyrin ($Pd(II)TMPy^{4+}$),[9] where the fast component k_f of the porphyrin triplet decay was pH-dependent. One explanation may be that the amino acid target moiety microenvironment is not sensitive to the pH change of the injected water. Probably, a portion of the hydrocarbon (heptane) chain may extend into the reverse micelle water pool, suggesting an oil environment for the tryptophan residue at the heptane−AOT interface.

Conclusions

Ground-state absorption spectra of $Pd(II)TMPy^{4+}$ and $Pd(II)TMPy^{4+}$ in AOT−heptane−H_2O reverse micelles indicated that electrostatic interactions of a tetracationic porphyrin with surfactant polar headgroups play a key role in determining the localization of the porphyrin molecules in reverse micelles. Particularly, the locus of solubilization was related to the micellar water composition. A critical micellar composition was found to be $w_0 \approx 10$. Below this critical value, the solubilization site was found to be dependent on w_0 and preferentially located near the micellar interface. Above $w_0 \approx 10$, the variation of absorption parameters (Soret band shift and maximum absorbance) with micellar water content suggested that the solubilization locus of the porphyrin molecule is independent of w_0. Furthermore, the saturation values of the absorption parameters (λ_{max}, Soret band shift $\Delta\lambda$) in reverse micelles differ considerably from those in bulk water, suggesting that the porphyrin remains located near the micellar interface.

Fluorescence spectra of the Zn-variant porphyrin showed characteristics similar to those observed from the ground-state investigation, namely (i) a critical micellar water composition of $w_0 \approx 10$; (ii) a w_0-dependent interfacial locus of solubilization below the critical micellar water composition; (iii) a similar porphyrin aqueous microenvironment in the vicinity of the water−AOT micelle interface above the critical micellar water composition; and (iv) the porphyrin molecule remains solubilized near the water−micelle interface and is not displaced toward the central pool upon saturating the reverse micelles with water.

Fluorescence from tryptophan residues of K_2WL_2 peptide incorporated in AOT−heptane−H_2O micelles revealed a critical micellar water composition that was similar to that observed from ground-state porphyrin absorption spectra measurements ($w_0 \approx 10$). Also, below $w_0 \approx 10$, the peptide microenvironment was found to be dependent on w_0, whereas above $w_0 \approx 10$, tryptophan fluorescence emission suggested a similar microenvironment. In addition, in the range of water composition investigated ($w_0 \approx 0.13-50$), the oligopeptide was found to be preferentially solubilized at the oil−AOT molecular interface.

Flash photolysis experiments showed that, in the presence of peptide in aqueous solution, $Pd(II)TMPy^{4+}$ triplet-state decay is strictly monoexponential. In reverse micelles, this decay was best described by the sum of two exponential terms. The fast decay component for both oligopeptides was found to be independent of the peptide concentration and dependent on the water-to-surfactant molar ratio (w_0). The slow decay component showed a linear dependence increase in value with inreasing peptide concentration. The fast contribution to the T_1 decay was associated with an electron transfer occurring in a discrete micelle between the target moiety (Y or W) and the photoexcited porphyrin molecule. The slow contribution of the decay was associated to molecular quenching during the micellar exchange process. The fast decay component was found to be pH-independent, suggesting a solubilization of the peptide molecule in a pH-independent environment near the oil−AOT molecular interface, where a portion of the hydrocarbon chain may extend into the aqueous phase.

Acknowledgment. Partial support for this work was provided by the National Institutes of Health, under NIH Grant No. CA91027. Dr. Mohamed Aoudia thanks Sultan Qaboos University for giving him the opportunity to spend a research summer leave at the Center for Photochemical Sciences at Bowling Green State University.

References and Notes

(1) Mines, G. A.; Bjerrum, M. J.; Hill, M. G. *J. Am. Chem. Soc*. **1996**, *118*, 1961.

(2) Scott, J. R.; Willie, A.; McLean, M. *J. Am. Chem. Soc*. **1993**, *115*, 6820.

(3) Zhou, J. S.; Tran, S. T.; McLendon, G.; Hoffman, B. M. *J. Am. Chem. Soc*. **1997**, *119*, 269.

(4) Zhou, J. S.; Granada, E. S. V.; Leontis, N. B.; Rodgers, M. A. J. *J. Am. Chem. Soc*. **1990**, *112*, 5074.

(5) Zhou, J. S.; Rodgers, M. A. J. *J. Am. Chem. Soc.* **1991**, *113*, 7728.
(6) Marcus, R. A. *J. Chem. Phys.* **1956**, *24*, 966.
(7) Jortner, J.; Bixon, M. In *Protein Structure: Molecular and Electronic Reactivity*; Austin, R., Buhks, E., Devault, D., Dutton, P. L., Frauenfelder, H., Gol′danskii, V. I., Eds.; Springer−Verlag: New York, 1987.
(8) Bixon, M.; Jortner, J.; Michel-Beyerle, M. E.; Ogrodnik, A. *Biochim. Biophys. Acta* **1989**, *977*, 273.
(9) Aoudia, M.; Rodgers, M. A. J. *J. Am. Chem. Soc.* **1997**, *119*, 12859.
(10) Aoudia, M.; Guliaev, A. B.; Leontis, N. B.; Rodgers, M. A. J. *Biophys. Chem.* **2000**, *83*, 121.
(11) Blundell, T.; Wood, S. *Annu. Rev. Biochem.* **1982**, *51*, 123.
(12) Bhattacharyya, K.; Basak, S. *Photochem. Photobiol.* **1995**, *62* (1), 17.
(13) Luisi, P. L.; Magid, L. J. *Rev. Biochem.* **1986**, *20*, 409.
(14) Willard, D. M.; Riter, R. E.; Levinger, N. E. *J. Am. Chem. Soc.* **1998**, *120*, 4151.
(15) Grand, D.; Dokutchaev, A. *J. Phys. Chem. B* **1997**, *101*, 3181.
(16) Walde, P.; Guiliani, A. M.; Boicelli, C. A.; Luisi, P. L. *Chem. Phys. Lipids* **1990**, *53*, 265.
(17) Onori, G.; Santucci, A. *J. Phys. Chem.* **1993**, *97*, 5430.
(18) Amico, P.; D'Angelo, M.; Onori, G.; Santucci, A. *Il Nuovo Cimento* **1995**, *17*, 1053.
(19) Zhukovskii, A. P.; Petrov, L. N.; Rovnov, N. V. *Zh. Strukt. Khim.* **1991**, *32*, 81.
(20) Christopher, D. J.; Yarwood, J.; Belton, P. S.; Hills, B. P. *J. Colloid Interface Sci.* **1992**, *152*, 465.
(21) Hauser, H.; Haering, G.; Pande, A.; Luisi, P. L. *J. Phys. Chem.* **1989**, *93*, 7869.
(22) Maitra, A. *J. Phys. Chem.* **1984**, *88*, 5122.
(23) Dunn, C. M.; Robinson, B. H.; Leng, F. J. *Spectrochim. Acta, Part A* **1990**, *46A*, 1017.
(24) Pileni, M.-P.; Zemb, T.; Petit, C. *Chem. Phys. Lett.* **1985**, *118*, 414.
(25) Zulauf, M.; Eicke, H. F. *J. Phys. Chem.* **1979**, *83*, 480.
(26) Belletete, M.; Lachapelle, M.; Durocher, G. *J. Phys. Chem.* **1990**, *94*, 7642.
(27) Hasegawa, M.; Sugimura, T.; Suzaki, Y.; Shindo, Y.; Kitahara, A. *J. Phys. Chem.* **1994**, *98*, 2120.
(28) Sarkar, N.; Das, K.; Datta, A.; Das, S.; Battacharyya, K. *J. Phys. Chem.* **1996**, *100*, 10523.
(29) Zhang, J.; Bright, F. V. *J. Phys. Chem.* **1991**, *95*, 7900.
(30) Karukstis, K. K.; Frazier, A. A.; Martula, D. S.; Whiles, J. A. *J. Phys. Chem.* **1996**, *100*, 11133.
(31) D'Angelo, M.; Fioretto, D.; Onori, G.; Palmieri, L.; Santucci, A. *Phys. Rev. E* **1996**, *54*, 993.
(32) Khougaz, K.; Gao, Z. S.; Eisenberg, A. *Langmuir* **1997**, *13*, 623.
(33) Hasegawa, M.; Sugimara, T.; Shindo, Y.; Kitahara, A. *Colloid Surf. A* **1996**, *109*, 305.
(34) Besso, K.; Uchida, T.; Yamanchi, A.; Shioya, T.; Terameae, N. *Chem. Phys. Lett.* **1997**, *264*, 381.
(35) Bhattacharyya, K.; Basak, S. *Biophys. Chem.* **1993**, *47*, 21.
(36) Grand, D.; Dokutchaev, A. *J. Phys. Chem. B* **1997**, *101*, 3181.
(37) Miller, S.; Janin, J.; Lesk, A. M.; Clothia, C. *Mol. Biol.* **1987**, *196*, 641.
(38) Michel, M.; Deisenhofer, J. *Curr. Top. Membr. Transp.* **1990**, *36*, 53.
(39) Henderson, R.; Baldwin, J. M.; Ceska, T. A.; Zemlin, F.; Beckmann, E.; Downing, K. H. *J. Mol. Biol.* **1990**, *213*, 899.
(40) Meers, P. *Biochemistry* **1990**, *29*, 3325.
(41) Hu, W.; Lee, K. C.; Cross, T. A. *Biochemistry* **1993**, *32*, 7035.
(42) Sciffer, M.; Chang, C. H.; Stevens, F. J. *Protein Eng.* **1992**, *5*, 213.
(43) Weiss, M. S.; Abele, U.; Weckesse, J.; Welte, W.; Schiltz, E.; Schulz, G. E. *Science* **1991**, *254*, 1627.
(44) Cowan, S. W.; Schirmer, T.; Rummel, G.; Steiert, M.; Ghosh, R.; Paupit, R. A.; Jansonius, J. N.; Rosenbusch, J. P. *Nature* **1992**, *358*, 727.
(45) Landolt-Marticorena, C.; Williams, K. A.; Deber, C. M.; Reitmeier, R. A. F. *J. Mol. Biol.* **1993**, *229*, 602.
(46) Saberwal, G.; Anderson, O. S. *Biophys. J.* **1996**, *70*, A181.
(47) Rihter, D. E.; Kenney, M. E.; Ford, W. H.; Rodgers, M. A. J. *J. Am. Chem. Soc.* **1993**, *115*, 8146.
(48) Luisi, P. L.; Giomini, M.; Pileni, M. P.; Robinson, B. H. *Biochim. Biophys. Acta* **1988**, *947*, 209.
(49) Biocelli, C. A.; Conti, F.; Giomini, M.; Guiliani, A. M. In *Physical Methods on Biological Membranes and Their Model Systems*; Conti, F., Blumberg, W. E., deGier, J., Pocchiari, F., Eds.; Plenum Press: New York, 1985; p 141.
(50) Akoum, F.; Parodi, O. *J. Phys.* **1985**, *46*, 1675.
(51) *Surfactants and Interfacial Phenomena*; Rosen, M. J., Ed.; John Wiley and Sons: New York, 1989.
(52) Teale, F. W. J.; Webber, G. *Biochemistry* **1957**, *65*, 476.
(53) Cowgill, R. W. In *Biochemical Fluorescence: Concepts 2*; Chen, R. F., Edelhoch, H., Eds.; Marcel Dekker: New York, 1976; p 441.
(54) Eicke, H. F.; Shepherd, J. C. W.; Steinemann, A. *J. Colloid Interface Sci.* **1976**, *56*, 168.
(55) Atik, S. S.; Thomas, J. K. *J. Am. Chem. Soc.* **1981**, *103*, 4376.
(56) Furois, J. M.; Brochette, P.; Pileni, M. P. *J. Colloid Interface Sci.* **1984**, *97*, 552.
(57) Brochette, P.; Pileni, M. P. *Nouveau J. Chem.* **1985**, *9*, 551.
(58) Kotlarchyk, M.; Chen, S. H.; Huang, J. S.; Kim, M. W. *Phys. Rev. A* **1984**, *29*, 2054.
(59) Dore, J. C.; North, A.; McDonald, J. A.; Howe, A. M.; Heenan, R. K.; Robinson, B. H. *Colloids Surf.* **1986**, *19*, 21.
(60) Robinson, B. H.; Steytler, J. C. W.; Tack, R. D. *Chem. Soc., Faraday Trans. I* **1979**, *75*, 81.
(61) Wong, M.; Thomas, J. K.; Gratzel, M. *J. Am. Chem. Soc.* **1976**, *98*, 2391.
(62) Rodgers, M. A. J.; Becker, J. C. *J. Phys. Chem.* **1980**, *84*, 2762.
(63) Pileni, M. P.; Gratzel, M. *J. Phys. Chem.* **1980**, *84*, 1822.
(64) Pileni, M. P.; Brochette, P.; Hickel, B.; Lerebours, B. *J. Colloid Interface Sci.* **1984**, *98*, 549.
(65) Thomas, J. K. *Acc. Chem. Res.* **1977**, *10*, 133.
(66) Wong, M.; Thomas, J. K.; Nowak, T. *J. Am. Chem. Soc.* **1977**, *99*, 4730.
(67) Smith, R. E.; Luisi, P. L. *Helv. Chim. Acta* **1980**, *63*, 2302.
(68) El Seoud, O. A. In *Reverse Micelles*; Luisi, P. L., Straub, E. E., Eds.; Plenum Press: New York, 1984; p 81.